

1. Large Helical Device (LHD) Project

The Large Helical Device (LHD) is a sizeable superconducting plasma confinement device employing a heliotron magnetic configuration. The objectives are to conduct academic research on the confinement of steady-state/high-temperature plasma for a comprehensive understanding of torus plasma. In the deuterium plasma experiment that started in 2017, we succeeded in generating plasma with both electron and ion temperatures reaching 100 million degrees. With this success, LHD research has entered a new phase, shifting to interdisciplinary research in 2021 and advanced study in 2022. We conducted the 24th experiment campaign for 14 weeks from the end of September to the end of December 2022.

The following four topical groups lead the LHD experiment by receiving support from domestic and international advisers, (1) Multi-ion plasma TG, (2) Turbulence TG, (3) Spectroscopy TG, and (4) Instability TG.

- The Multi-ion plasma TG deals with multi-ion transport, which is one of the crucial issues in a magnetically confined fusion reactor. The key research phrases are (i) mock test of sustainable burning and (ii) multi-ion transport (circulation) in terms of core-edge-wall coupling.
- The Turbulence TG emphasizes being aware of the intervention of turbulence in various physical phenomena occurring in LHD plasmas and actively investigates the relationships among them, particularly focusing on the turbulence interaction in PHASE and REAL space.
- The Spectroscopy TG addresses the following topics by employing various spectrometers with ranges from visible to X-ray. (i) Collisional-radiative properties of heavy ions, (ii) neutral particle transport in divertor and plasma boundary regions, and (iii) the non-Maxwell and anisotropic velocity distribution function of particles.
- The Instability TG deals with topics on (i) wave-particle interaction, (ii) abrupt events, (iii) transition phenomena, and (iv) topological effects. Also, the TG will cover the basic topic related to high-beta, MHD, and energetic-particle physics.

In 2022, 397 domestic and international researchers were registered in the LHD experiment groups, and 209 experiment proposals were submitted to each topical group, as shown in Figure. Many research results were achieved during the 24th experiment campaign in 2022, as described in the following URL.

https://www-lhd.nifs.ac.jp/pub/Science_en.html

Significant results were made public through press releases and introduced on the NIFS web page at the following URL.

https://www.nifs.ac.jp/en/news/index_list.html

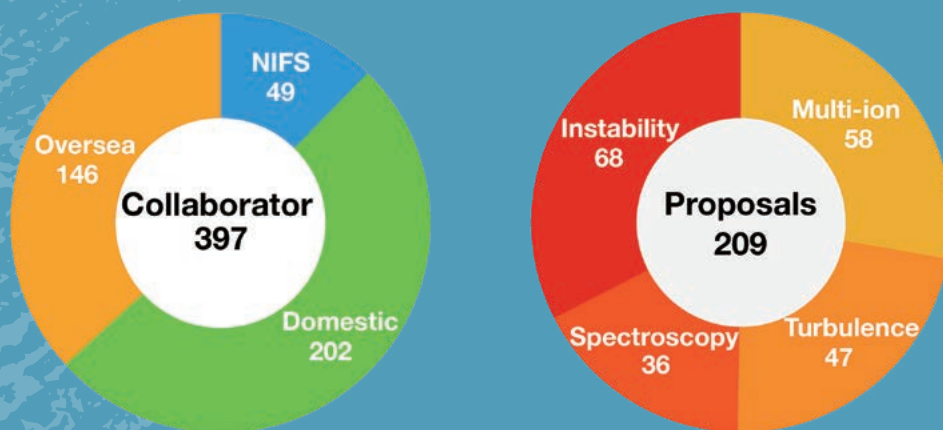


Figure: (left) number of domestic and international researchers, and (right) number of Proposals

The 24th experiment campaign is the final one of a ten year venture as the Project to Promote Large Scientific Frontiers of MEXT. In the coming years, the LHD will be born again in the framework of the Academic Research Platform of MEXT as a three year project from 2023 to 2025. The Academic Research Platform, utilizes the LHD, which can stably produce high-temperature plasma, as an interdisciplinary research platform, conduct international joint research to explore the principles of various complex phenomena common not only to fusion but also to space and astronomical plasmas.

(R. Sakamoto)

Multi-ion Plasma

Highlight

Data-Driven Control for Radiative Collapse Avoidance [1]

A data-driven predictor of radiative collapse, which is the major cause of sudden plasma termination in stellarator-heliotron devices, has been developed by means of a machine-learning technique. The control system with this predictor has successfully demonstrated the avoidance of radiative collapse and a secure high-density operation in the LHD.

A support vector machine (SVM), which is one of the machine-learning models, has been trained to distinguish whether the plasma is “close-to-collapse” or “stable” based on high-density experiment data in the LHD. The predictor has been designed to calculate the “collapse likelihood”, which is 0 when the plasma is stable and close to unity when the plasma approaches collapse, from plasma parameters featured by the trained SVM [2].

The schematic diagram of the collapse-avoidance control system is shown in Fig. 1. The control system receives signals of plasma density, temperature, and impurity line emission intensities, and calculates the collapse likelihood in real-time. When the likelihood approaches unity, a control signal is sent to the EC heating system to inject additional heating power and to the gas-puff controller to stop fueling. When the likelihood decreases, the control signal is turned off.

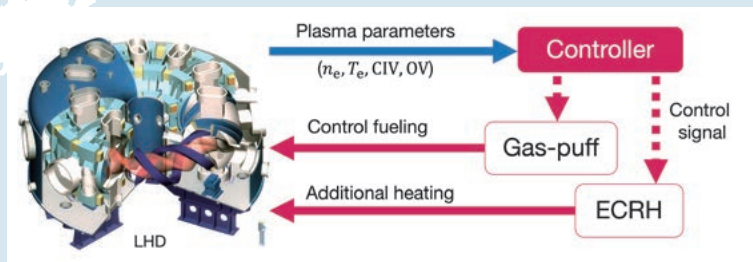


Fig. 1 Schematic diagram of the collapse avoidance control system.

Figure 2 shows the discharges with and without the collapse-avoidance control in LHD experiments. When the density increased, the radiative collapse occurred at the initial phase in the discharge without the control. In the discharge with the control, the collapse in the initial phase was avoided by regulating gas-puff and ECH. Consequently, the discharge evolved to a high density of $1.2 \times 10^{20} \text{ m}^{-3}$ successfully while avoiding radiative collapse. This is the first reported work to control stellarator-heliotron plasma with avoidance of radiative collapse by means of a machine-learning model.

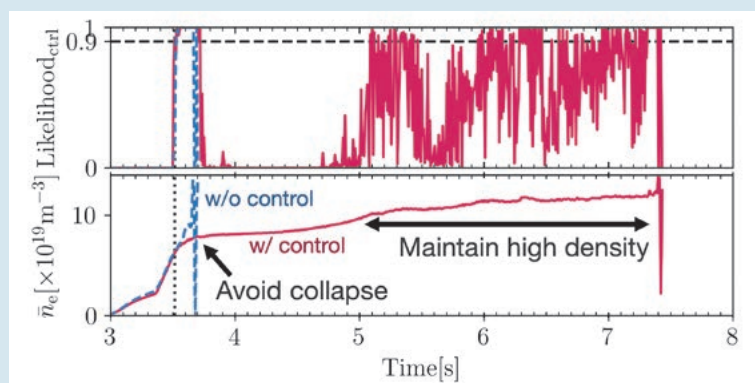


Fig. 2 The collapse likelihood (upper) and line-averaged electron density (bottom) in the discharges with (red) and without (blue) the collapse avoidance control system. The dashed horizontal line in the top panel and the dotted vertical line show the threshold value and the time when the likelihood initially exceeded the threshold.

[1] T. Yokoyama *et al.*, “Data-Driven Control for Radiative Collapse Avoidance in Large Helical Device,” *Plasma and Fusion Research* **17**, 2402042 (2022).

[2] T. Yokoyama *et al.*, “Data-Driven Approach on the Mechanism of Radiative Collapse in the Large Helical Device,” *Plasma and Fusion Research* **16**, 2402010 (2021).

Non-contact thermometer to measure the temperature of ultra-high temperature plasma –Successful observation of multi-temperature anisotropic energetic ions [1]

In fusion plasmas, α -particles generated by the fusion reaction between deuterium and tritium in the plasma sustain the burning of the plasma and generate energy. Therefore, to realize nuclear fusion, it is necessary to know and control the state of the energetic α -particles generated in the high-temperature plasma. Although it is challenging to measure α -particles in the high-temperature plasma, we considered non-contact measurement and started the development of collective Thomson scattering (CTS) measurement using electromagnetic waves.

The research team has reported on a method for evaluating ion temperature and velocity distribution using the scattering phenomena of millimeter electromagnetic waves [2]. This study developed a high-precision in-situ calibration method for CTS measurements and applied it to temperature measurements in the Large Helical Device (LHD) plasmas. Conventionally, a radiation of electromagnetic waves in plasma is used to calibrate the receiver for CTS measurements. However, the local position of the emitted radiation was inaccurate due to the refraction, and it was necessary to determine the location. To solve this problem, we combined a ray tracing calculation of electromagnetic waves with the calibration of receiver sensitivity by electron radiation. As a result, we succeeded in dramatically improving the reproducibility of the scattering spectrum. Furthermore, we have demonstrated that in-situ calibration is possible using this method simultaneously with actual temperature measurements.

Using this method, we observed the scattering spectrum at the center of the LHD plasma by the CTS measurement. As expected from the model calculation of the scattering spectrum, the observed spectrum has an asymmetric shape (asymmetric when there is a population of ions with different velocities in the positive and negative directions of v_{\parallel} in the figure). This asymmetry indicated complex confinement of anisotropic ions with parallel and perpendicular velocities to the magnetic field lines and was found to be due to plasma heating.

These results are essential for the study of confinement physics of alpha particles to maintain a self-burning state in fusion plasmas. Furthermore, since in-situ calibration is also possible, it is expected to be widely used as a calibration and analysis method for electromagnetic heating devices and millimeter-wave measurement devices used in fusion power generation.

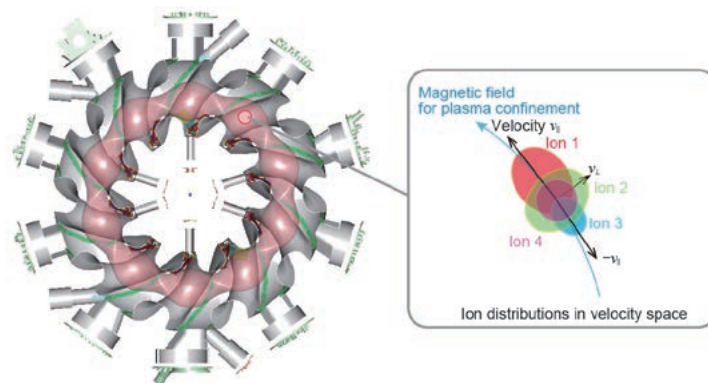


Fig. 1 LHD and high temperature plasma

Plasma confined in the magnetic field of the LHD has the shape of a twisted donut. Using a non-contact thermometer, we measured the temperature of the high-temperature plasma core by injecting millimeter waves and measuring their scattered light. The results show that the velocity spread of the ion population, which corresponds to the ion temperature, has a variety of directions: along the confinement magnetic field (ion 1), in the opposite direction (ion 3), perpendicularly (ion 2), and a thermalized isotropic component (ion 4). This complex state can be attributed to plasma heating to generate and maintain the high-temperature plasma.

[1] M. Nishiura, S. Adachi, K. Tanaka, N. Kenmochi, T. Shimozuma, R. Yanai, T. Saito, H. Nuga, R. Seki, "Collective Thomson scattering diagnostic with *in situ* calibration system for velocity space analysis in large helical device" Rev. Sci. Instrum. **93**, 053501 (2022). <https://doi.org/10.1063/5.0079296>

[2] M. Nishiura *et al.*, Nucl. Fusion **54**, 023006 (2014).

(M. Nishiura)

Validation of plasma-wall interaction simulation code ERO2.0 by analysis of tungsten migration in the open divertor configuration

Tungsten migration in an open divertor configuration in the LHD was analyzed for validating the three-dimensional plasma-wall interaction simulation code ERO2.0 [1]. In the experimental campaign in Fiscal Year 2008, a tungsten-coated divertor plate was installed on the right-divertor plate array in the inboard side of the torus. Figure 1 (a) shows a three-dimensional grid model for analyzing the tungsten migration in an open divertor configuration for the ERO2.0 code. The simulation reproduced a measured localization of tungsten migration near a tungsten-coated divertor plate along the divertor plate array. Figure 1 (b) indicates the simulation of the integrated net tungsten areal density profile on the carbon divertor plates. The simulation qualitatively reproduced the experimental results of high tungsten areal density in the private side on a carbon divertor plate (“R18”) installed next to the tungsten-coated divertor plate (shown by a gray arrow). It showed that it was mainly caused by tungsten prompt redeposition in plasma discharges for low magnetic fields in a counterclockwise toroidal direction. Figure 1 (c) presents the integrated net tungsten areal density profile along the black lines on four selected carbon divertor plates (“R20”, “R18”, “R16”, and “R8” shown in Figure 1 (b)). The measured tungsten areal densities at three positions (“a”, “b”, and “c”) on the four divertor plates are shown as red circles. While the simulation reproduced the above two experimental results, it disagreed with the measurement of low tungsten areal density on the plasma-wetted areas on the divertor plates. It demonstrated that the actual erosion rate of the redeposited tungsten in the plasma-wetted areas on the divertor plates should be much higher than that adopted in the ERO2.0 simulation code [2].

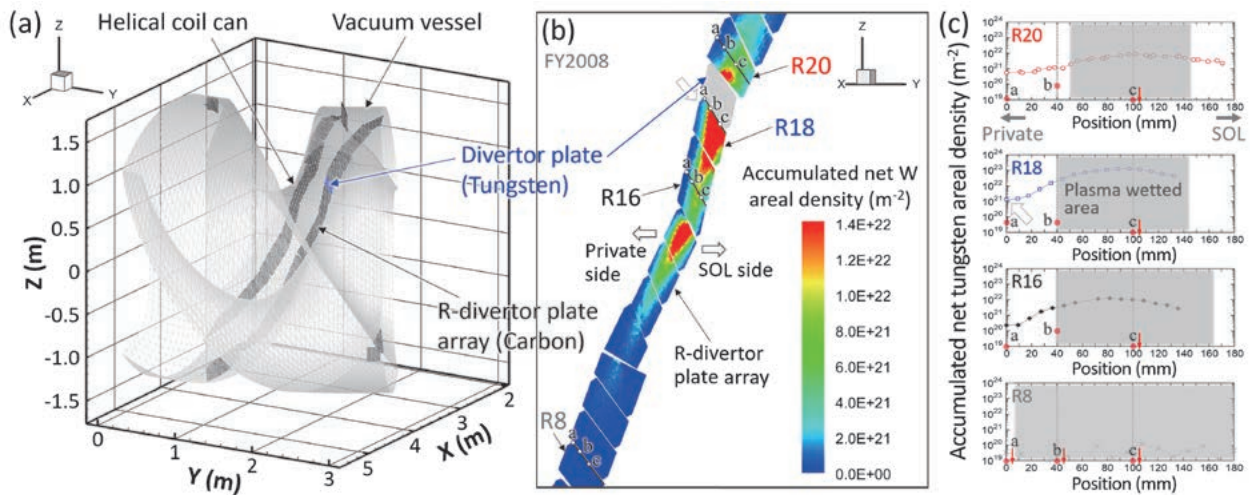


Fig. 1 (a) A three-dimensional grid model for analyzing the tungsten migration in the open divertor configuration in the LHD for one helical pitch angle (36° in toroidal direction) for the ERO2.0 code. (b) The simulation of the integrated net tungsten areal density profile on the carbon divertor plates installed along the right divertor plate array in the experimental campaign (FY2008). (c) The integrated net tungsten areal density profiles along the black lines on the four carbon divertor plates shown in Figure (b). The measured tungsten areal densities at the three positions (“a”, “b”, and “c”) on the four selected divertor plates (“R20”, “R18”, “R16”, and “R8”) indicated as red circles. Gray-shaded regions show the plasma-wetted areas on the divertor plates.

[1] J. Romazanov *et al.*, Nucl. Mater. Energy **18**, 331 (2019).

[2] M. Shoji *et al.*, Nucl. Mater. Energy **33**, 101294 (2022).

Extraction of three-dimensional structure of radiative cooling from two-dimensional radiation images in Large Helical Device [1]

Three-dimensional localization of radiative cooling due to nitrogen (N_2) seeding for divertor heat load reduction has been detected experimentally. A fusion reaction occurs by confining high-temperature plasma exceeding 100 million Celsius degrees in fusion reactors. Since the flow from the core plasma with a high temperature to a place called the “divertor” on the wall of the device is huge, it is necessary to mitigate the local heat load of the divertor. Therefore, an operational method called “divertor detachment” is being studied, in which impurities are injected from outside the plasma and the heat load is dispersed as radiation. In the LHD, we performed experiments on the divertor detachment.

Although toroidally-symmetric divertor heat load reduction is preferable for fusion reactors, toroidally asymmetric reduction is observed in various torus devices. The localization of radiative cooling along some magnetic field lines is implied as the reason for the asymmetry, however, the localization has not been measured in previous works. In this research, a three-dimensionally localized structure was extracted using principal component analysis (PCA) from two-dimensional radiation images measured with an InfraRed imaging Video Bolometer (IRVB). By applying PCA to 34 images each in N_2 seeded plasmas with toroidally-asymmetric reduction (Fig. 1 (a)) and in neon (Ne) seeded plasmas with toroidally-symmetric reduction (Fig. 1 (b)), a radiation feature in N_2 seeded plasmas was found as one of the principal components (Fig. 1 (c)). The three-dimensional transport code EMC3-EIRENE indicated that the ionization in one of the divertor legs was enhanced in nitrogen seeding compared with Ne seeding due to the difference in the first ionization energy. The magnetic field lines from the divertor leg were along the extracted radiation structure and were terminated by the divertor where the heat load decreased due to the N_2 seeding (Fig. 2). These results indicate that the three-dimensionally localized structure of radiative cooling was detected experimentally.

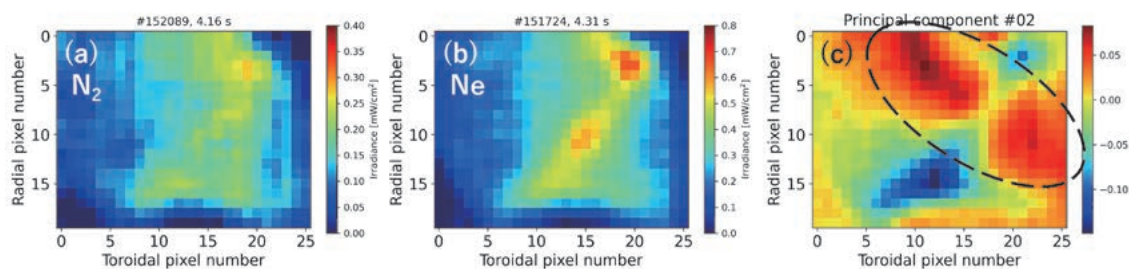
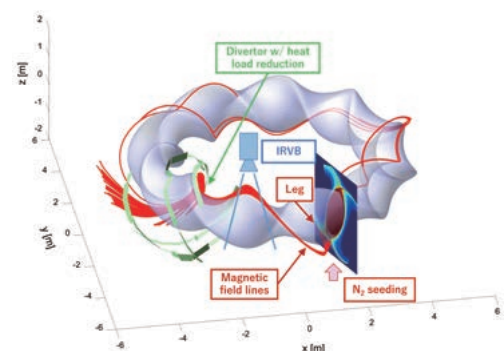


Fig. 1 Typical radiation images of IRVB in (a) N_2 and (b) Ne seeded plasmas. (c) Principal component extracted from 68 images of N_2 and Ne seeded plasmas. A dashed ellipse indicates the localized structure in N_2 seeded plasmas.

Fig. 2 Magnetic field lines traced from the divertor leg of the N_2 seeding port with the field of view of IRVB and divertor plates.



[1] K. Mukai *et al.*, Nucl. Mater. Energy **33**, 101294 (2022).

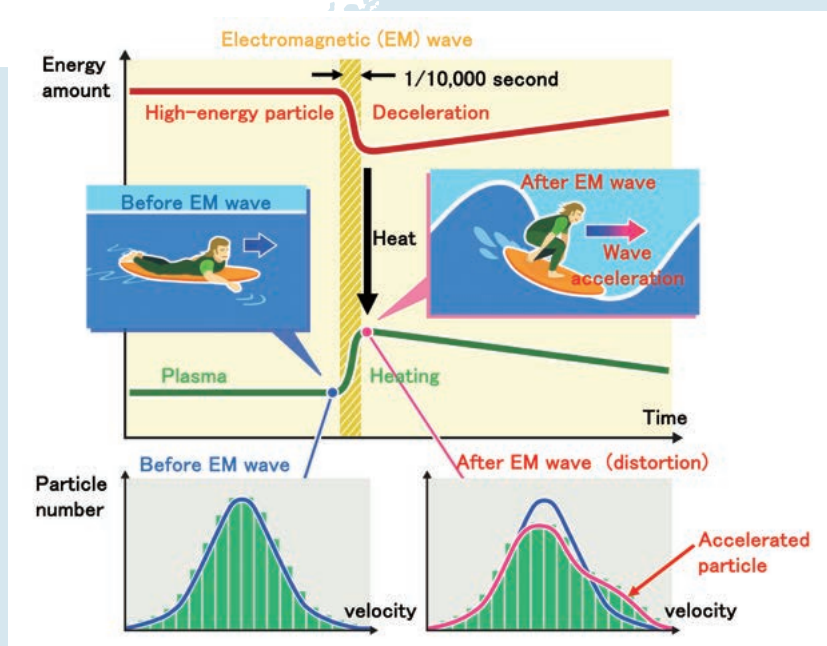
TG2: Turbulence Topical Group

Highlight

Direct observation of mass-dependent collisionless energy transfer via Landau and transit-time damping

There has been no method to directly measure the collisionless energy transfer from high-energy ions to bulk ions through the electromagnetic waves generated inside plasma. Therefore, it is not known whether this process exists. To directly measure the heating process, it is necessary to determine the time variation of the velocity distribution, which indicates which velocity ions are present and in what proportion. A high-speed charge exchange spectroscopy system has been developed to measure the time variation of the velocity distribution of plasma ions at an ultrahigh-speed of 10 kHz.

In the LHD, experiments are being conducted to investigate plasma self-heating using a high-speed neutral beam that simulates high-energy Helium from nuclear fusion reactions. In this experiment, to simulate self-heating, a newly developed measurement system was used to measure in detail the time variation of the velocity distribution of plasma ions. As a result, it was discovered for the first time in the world that the plasma was heated due to the slowing down of the high-speed beam and the distortion of the velocity profile of the plasma ions caused by the generation of electromagnetic waves inside the plasma (see Figure). The reason for this distortion of the velocity profile was found to be that the energy of the high-speed beam was transferred to the electromagnetic wave through a process called Landau/transit-time damping, and the energy of the electromagnetic wave was transferred to the plasma ions. In other words, the electromagnetic waves carried the energy of the high-speed beam to the plasma and heated it, which is basically the same process as so-called alpha-channeling in fusion plasma. [1]



Heat is carried by electromagnetic waves, which simultaneously slow down the high-speed particle beam (red line) and heat up the plasma particles (green line). Distortion of the velocity distribution is observed due to the acceleration of the particles as a result of the electromagnetic waves.

[1] K. Ida *et al.*, *Communications Physics* **5**, 228 (2022).

Isotope effect in the internal transport barrier threshold condition

As a long-standing mystery in the magnetically confined plasma community, the background physics of the hydrogen isotope effect has been intensively studied. The isotope effect in the threshold power necessary for triggering H-mode transitions is experimentally demonstrated, which is favorable to plasmas with larger isotope mass [1]. Such an observation is routinely obtained in different tokamak devices, but the knowledge concerning stellarators is scarcely accumulated in literature due to the lack of experimental cases. In the Large Helical Device (LHD), the hydrogen isotope effect on the transition threshold for the electron internal transport barrier (electron-ITB) is discovered.

In the LHD, the electron-ITB is produced typically in plasmas with low density and high electron cyclotron resonance heating (ECH) power. The hydrogen isotope effect in the electron-ITB is assessed based on a perturbative experiment. In a steady state plasma discharge, the ECH heating power is modulated and the response in the electron temperature gradient is observed. When the base electron density is sufficiently high, the modulation amplitude in the electron temperature gradient is maintained to be small and does not depend on line-averaged density. However, it monotonically increases as the line averaged density is decreased in a lower density range,

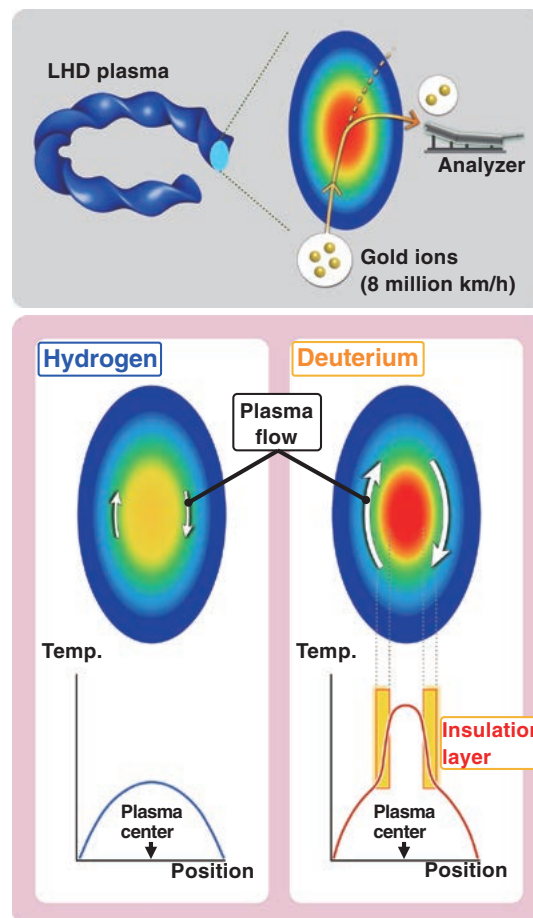


Fig. 1 Top: Plasma measurement using a heavy ion beam probe. A high-speed beam of gold ions is injected into the plasma to measure the flow generated inside it. Bottom left: Hydrogen plasma has weak flow and no insulation layer. Bottom right: Deuterium plasma has strong flow and a high-performance insulation layer.

which is considered to be due to the transient electron-ITB formation/deformation synchronizing the modulation ECH. The threshold density for the electron-ITB transition is higher in the deuterium case, i.e., the electron-ITB is easily formed in the heavier hydrogen isotope fuel. This isotope effect is found to be predominantly caused by a branch transition in local electron thermal diffusivity. In a higher density range, the local electron thermal diffusivity follows the $\bar{n}_e^{-1.2}$ trend, likely due to the density stabilization effect in global confinement scaling. Once the density crosses the electron-ITB threshold, the local electron thermal diffusivity drops off from the $\bar{n}_e^{-1.2}$ trend [2]. Unlike the local transport property, the nonlocal contribution scarcely has any meaningful difference in deuterium and hydrogen plasmas [2,3]. According to the heavy ion beam probe (HIBP) data, it is found that a central radial electric field transition occurs at a higher density level in deuterium plasmas [4], as shown in Fig. 1, which is likely responsible for the isotope effect in the electron-ITB formation. The fact that self-organized radial electric field criticality has a susceptibility to plasma ion mass is systematically pointed out for the first time.

[1] C. F. Maggi *et al.*, Plasma Phys. Control. Fusion **60**, 014045 (2017).

[2] T. Kobayashi *et al.*, Nucl. Fusion **60**, 076015 (2020).

[3] T. Kobayashi *et al.*, Plasma Fusion Res. **15**, 1402072 (2020).

[4] T. Kobayashi *et al.*, Sci. Rep. **12**, 5507 (2022).

(T. Kobayashi)

Discovery of fast moving plasma turbulence: New insights into the understanding of fusion plasma turbulence

To achieve a fusion power plant, a plasma of more than 100 million degrees Celsius must be stably confined in a magnetic field and maintained for a long time. In the Large Helical Device (LHD), it has been discovered for the first time that when heat escapes from the plasma, turbulence moves faster than heat [1]. The characteristic of this turbulence makes it possible to predict changes in plasma temperature, and it is expected that the observation of turbulence will lead to the development of a method for real-time control of plasma temperature in the future.

In a high-temperature plasma confined by a magnetic field, “turbulence” – a flow with vortexes of varying sizes – is generated. This turbulence disturbs the plasma and the heat from the confined plasma flows outwards, causing the plasma temperature to drop. To solve this problem, it is necessary to understand the characteristics of heat and turbulence in plasma. However, turbulence in plasmas is so complex that we still do not fully understand it. In particular, how the generated turbulence moves in the plasma is not well understood because it requires instruments that can measure the time evolution of minute turbulence with high sensitivity and extremely high spatial and temporal resolution.

A “barrier” can form in the plasma that blocks the transport of heat from the center outwards. The barrier creates a strong pressure gradient in the plasma and generates turbulence. We have developed a method to break this barrier by designing a magnetic field structure (Fig. 1). This method allows us to focus on the heat and turbulence that flow strongly when the barrier is broken, and to study their relationship in detail. We then use electromagnetic waves of different wavelengths to measure the changing temperature and heat flow of electrons and millimeter-sized fine turbulence with the world’s highest accuracy. Heat and turbulence were previously known to move almost simultaneously at a speed of 5,000 kilometers per hour, about the speed of an airplane, but this experiment

led to the world's first discovery of turbulence moving ahead of heat at a speed of 40,000 kilometers per hour. The speed of this turbulence is close to that of a rocket.

This research has advanced our understanding of turbulence in fusion plasmas. The new property of turbulence, that it moves much faster than heat in a plasma, suggests that we may be able to predict plasma temperature changes by observing predictive turbulence. In the future, we expect to develop methods to control plasma temperatures in real time.

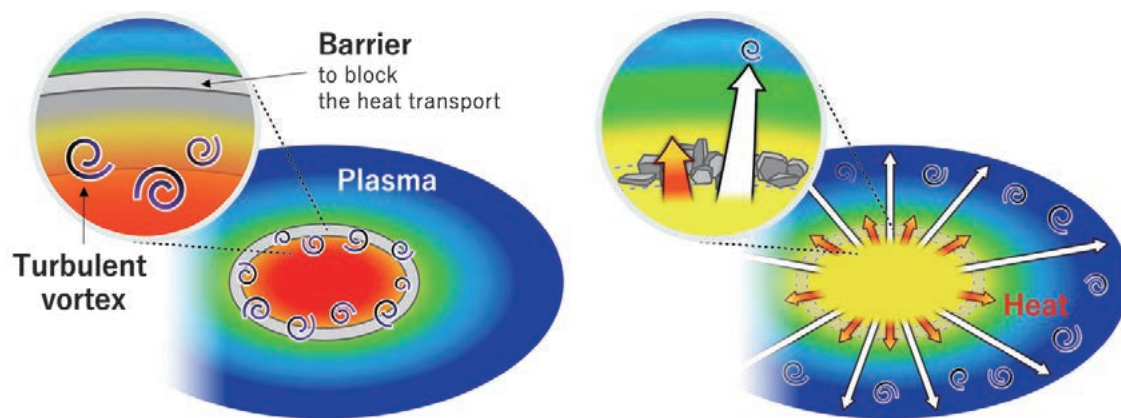


Fig. 1 Figure (left): Creating a barrier in the plasma to confirm the heat inside. (Right): Breaking the barrier revealed turbulence moving faster than the heat escaping from inside the plasma.

[1] N. Kenmochi *et al.*, *Scientific Reports* **12**, 6979 (2022).

(N. Kenmochi)

Plasma Spectroscopy

Highlight

Electron temperature and density measurement by Thomson scattering with a high repetition rate laser of 20 kHz on LHD [1]

In order to measure the electron temperature (T_e) and density (n_e) during fast phenomena in plasmas, a high-repetition frequency Nd:YAG laser and fast digitizers are installed in the Thomson scattering system in the LHD. This laser has been newly developed under the collaboration of NIFS and the University of Wisconsin-Madison, based on a pulse-burst technique and can be operated with two repetition frequencies, one of which is 1 kHz with 30 laser pulses and the other is 20 kHz with 100 laser pulses.

The temporal development of the scattered light signals is acquired by the fast digitizers of the switched-capacitor type with 1 GS/s. The minimum read-out time of these digitizers is shorter than 50 μ s in order that the signals in the 20 kHz operation of the laser can be acquired. Since the data which are obtained by the switched-capacitor type digitizers require some kinds of corrections, the cell-size and peak corrections, are made. Some methods of the evaluation of the background level and the time integration are developed. After these data processing procedures, the T_e profiles are derived by the χ^2 -method. n_e is evaluated with the results of the Raman scattering calibration.

Figure 1 shows temporal development of the spatial profiles of T_e (red), n_e (blue) and electron pressure (yellow) after a pellet injection in the LHD plasma. n_e started to increase at $t = 8.00275$ s (Fig. 1b) from the outside of the torus. The low T_e region where $T_e < 0.3$ keV penetrated the core region of the plasma. In Fig. 1c, quite high n_e was observed in the torus outer region. The temporal development of T_e and n_e within 1 ms was observed in detail by this diagnostic.

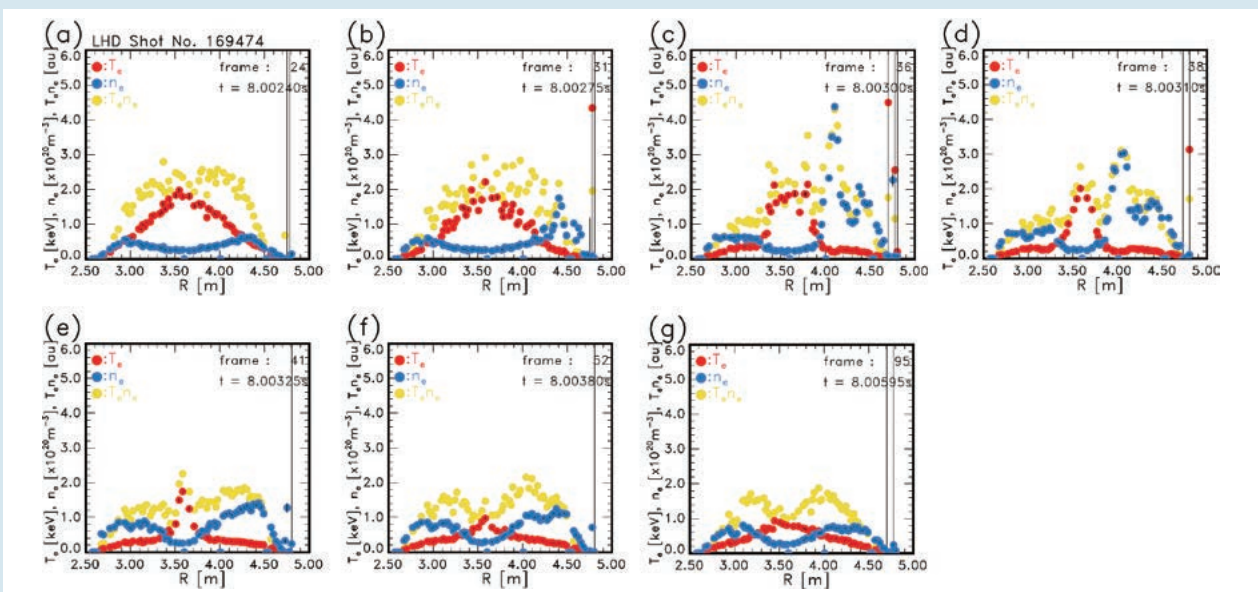


Fig. 1 Spatial profiles of electron temperature (red), electron density (blue) and electron pressure (yellow) of a pellet injected plasma in the LHD. They are measured by the Thomson scattering system with a high-repetition rate Nd:YAG laser of 20 kHz.

[1] H. Funaba *et al.*, Sci. Rep. **62**, 15112 (2022).

(H. Funaba and R. Yasuhara)

Experimental Study on Boron Distribution and Transport at Plasma-Facing Components during Impurity Powder Dropping in the Large Helical Device [1]

We performed spatially-resolved spectroscopic measurements of emissions by boron ions and BH molecules (Fig. 1). As a result, a concentration of BH and B^+ was confirmed in the divertor region during impurity powder dropping experiments with boron powder (Fig. 2), which suggest successful observation of boron deposition and desorption processes on the divertor plate. By comparing H γ emissions with and without boron injection, neutral hydrogen shows uniform reduction in the SOL region, whereas less reduction of neutral hydrogen is confirmed in the divertor region. Although emissions from BH and B^+ increased linearly, those by B^0 and B^{4+} became constant after the middle of the discharge (Fig. 3). Continuous reduction of carbon density in the core plasma was confirmed even after B^0 and B^{4+} became constant. The results may show reduction of hydrogen recycling and facilitation of impurity gettering by boron in the divertor region and thus effective real-time wall conditioning.

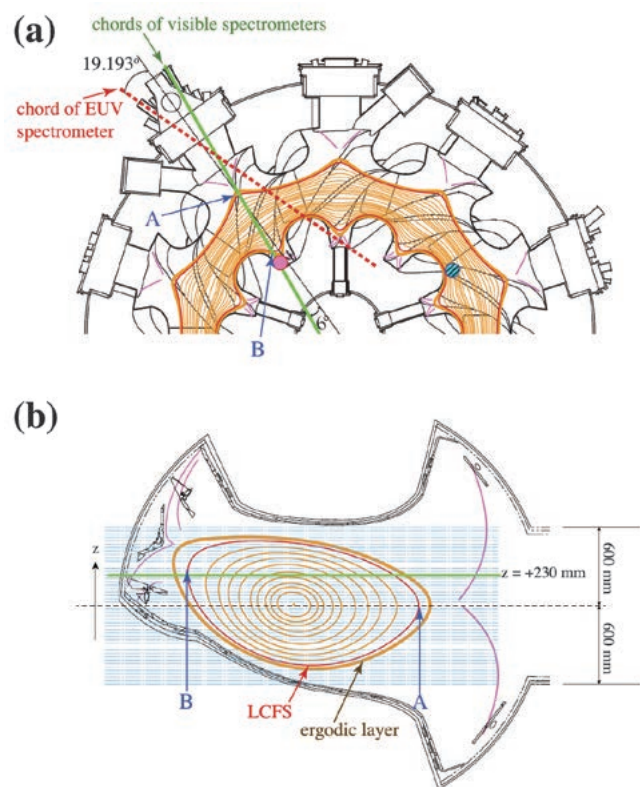
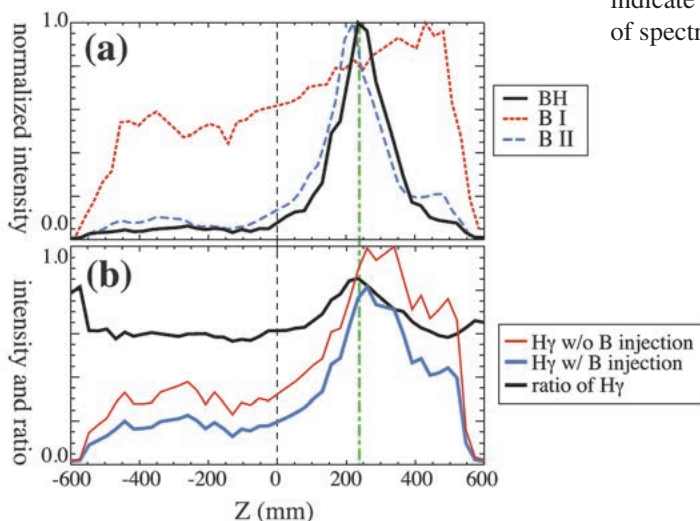


Fig. 1 Line of sight of visible and EUV spectrometers. (a) Half equatorial cross section of LHD. Positions of powder dropper (blue circle, hatched) and Langmuir probe array examined in this study (pink circle) also shown. (b) Plane of chords of visible spectrometers. In (a) and (b), A and B indicate outer and inner edges of LCFS in plane of chords of spectrometers.

Fig. 2 (a) Observed emission distributions of BH, B I, and B II at $t = 6.0$ s. (b) Observed emission distributions of H γ during shot without and with boron injection at $t = 6.0$ s. Ratio of H γ intensities between two discharges with and without boron injection at $t = 6.0$ s shown as black curve. Vertical green dot-dashed line indicate position of divertor viewing chord.

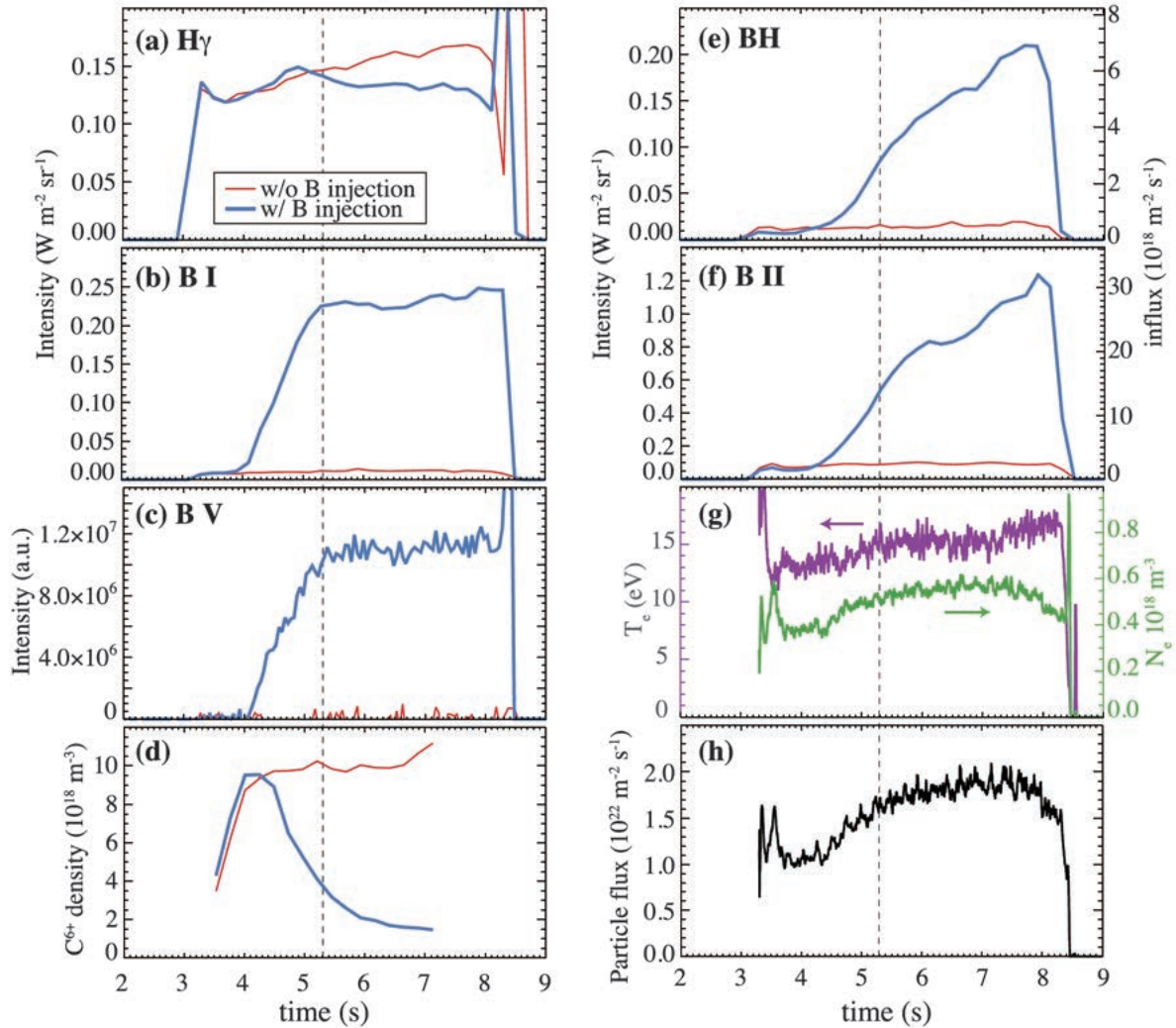


Fig. 3 Temporal evolutions of intensities of (a) $H\gamma$, (b) B I, (c) B V, (d) C^{6+} density on magnetic axis measured by CXS, (e) BH, (f) and B II in discharges without and with boron injection (thick blue), (g) Te and Ne on divertor, and (h) particle flux onto divertor. (a), (b), (e) and (f) are data in divertor viewing chords. Vertical dashed lines show $t = 5.3$ s, after which flattening structure appeared in evolutions of B I and B V.

[1] T. Kawate *et al.*, Nuclear Fusion **62**, 126052 (2022).

(T. Kawate)

Detailed Analysis of Spectra from Ga-like Ions of Heavy Elements Observed in High-Temperature Plasmas [1]

Extreme ultraviolet (EUV) and soft X-ray emission spectra from highly charged heavy ions are of great interest in various research fields, including nuclear fusion and industrial light source applications, as well as basic atomic physics. Among a wide range of ion stages, gallium-like (Ga-like) ions give rise to relatively simple spectral features because of their simple electron configuration of the ground state: $[\text{Ar}]3d^{10}4s^24p$. However, experimental and theoretical investigations of them are still incomplete.

This study focuses on the atomic number (Z) dependence of spectra from Ga-like ions of heavy elements based on the spectral data which have systematically been recorded in high-temperature plasmas produced in the Large Helical Device (LHD). A small amount of heavy elements are injected into LHD plasmas, mainly by a tracer-encapsulated solid pellet (TESPEL), and the temporal evolutions of EUV/soft X-ray emission spectra are recorded by multiple grazing incidence spectrometers. The measured wavelengths are compared with theoretical values calculated with a multi-configuration Dirac Fock code: GRASP92. Consequently, Z dependent wavelengths of several prominent transitions of Ga-like ions have successfully been obtained. Some of them have been experimentally identified for the first time in the LHD.

It has already been reported that the energy level crossing of $[\text{Ar}]3d^{10}4s^24d$ and $[\text{Ar}]3d^{10}4s4p^2$ configurations takes place between $Z=62$ and 63 because of a strong configuration interaction [2]. The present study gives additional results of Z dependence analysis for the other transitions. In particular, the present study has successfully identified the lines due to magnetic dipole (M1) transitions between doublets of the ground configuration (Fig. 1). The Z dependence of the measured wavelengths for Z from 63 onward is lined up along a single smooth curve and is in very good agreement with the calculation. The wavelengths of these M1 lines correspond to the energy splitting due to spin-orbit interaction. In this respect, the present results provide some fundamental data to study atomic physics specific to highly charged heavy ions: Z -dependent configuration interaction and spin-orbit interaction.

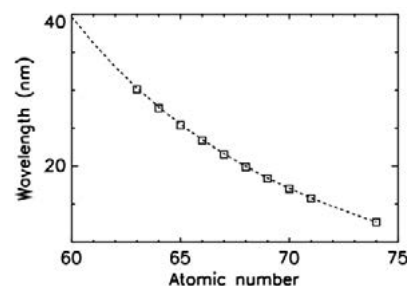


Fig. 1 Z dependence of the wavelength of the magnetic dipole (M1) transition from $(4p_+)_{3/2}$ to the ground state $(4p_-)_{1/2}$ of Ga-like ions. The measured and calculated wavelengths are shown by squares and a broken line, respectively.

[1] C. Suzuki *et al.*, *Atoms* **11**, 33 (2023).

[2] F. Koike *et al.*, *Phys. Rev. A* **105**, 032802 (2022).

(C. Suzuki)

EUV/VUV Spectroscopy for the Study of Carbon Impurity Transport in Hydrogen and Deuterium Plasmas in the Edge Stochastic Magnetic Field Layer of the Large Helical Device [1]

The ergodic layer in the Large Helical Device (LHD) consists of stochastic magnetic fields exhibiting a three-dimensional structure that is intrinsically formed by helical coils. Spectroscopic diagnostics were employed in the extreme ultraviolet (EUV) and vacuum ultraviolet (VUV) wavelength ranges to investigate emission lines of carbon impurities in both hydrogen (H) and deuterium (D) plasmas, aiming to elucidate the impact of distinct bulk ions on impurity generation and transport in the edge plasmas of the LHD. Figure 1 exhibits the dependence of carbon line intensity on the line-averaged electron density for different charge states: (a) CIII (977.03 Å, 2s²-2s2p), (b) CIV (1548.02 Å, 2s-2p), (c) CV (40.27 Å, 1s²-1s2p), and (d) CVI (33.73 Å, 1s-2p), normalized by the line-averaged electron density. The emission intensity of carbon ions in all charge states is enhanced in deuterium discharges. This enhancement can be attributed to the higher sputtering rate of carbon materials by deuterium plasma compared to hydrogen plasma, resulting in an increased generation of carbon impurities from the divertor plates. Figure 1(e) presents a line ratio of CV/CIV as an indicator of the impurity screening effect, where smaller values indicate a stronger impurity screening effect. A comparison between deuterium and hydrogen plasmas in Figure 1(e) reveals that the impurity screening effect is more pronounced in deuterium plasmas. A Doppler profile measurement of the second order of CIV line emission (1548.20 × 2 Å) was attempted using a 3 m normal-incidence VUV spectrometer in the edge plasma at a horizontally elongated plasma position. The flow velocity reaches its maximum value close to the outermost region of the ergodic layer, and the observed flow direction

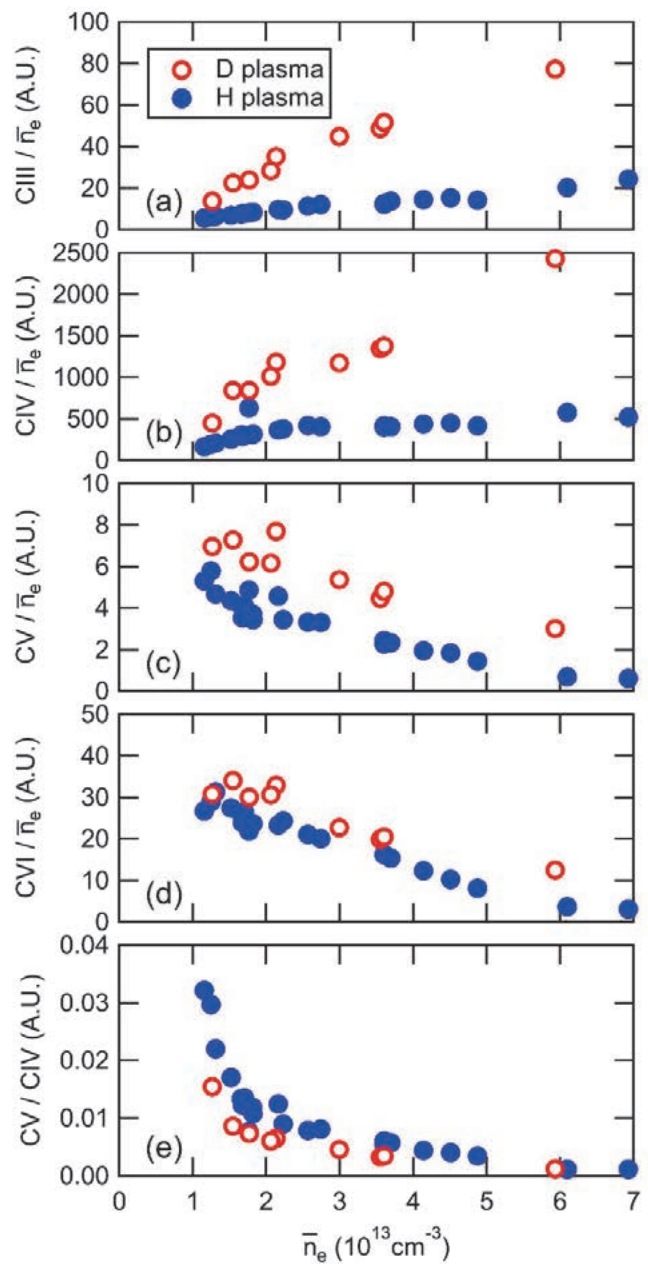


Fig. 1 Line-averaged electron density dependence of line intensity of (a) CIII, (b) CIV, (c) CV, (d) CVI normalized by the electron density and (e) line ratio CV/CIV for deuterium and hydrogen discharges.

aligns with the friction force in the parallel momentum balance. The flow velocity increases with the electron density in H plasmas, suggesting that the friction force becomes more dominant in the force balance at higher density regimes. This leads to an increase in the impurity flow, which can contribute to the impurity screening. In contrast, the flow velocity in the D plasma is smaller than that in the H plasma. The difference in flow values between D and H plasmas, when the friction force term dominates in the momentum balance, could be attributed to the mass dependence of the thermal velocity of the bulk ions (Fig. 2).

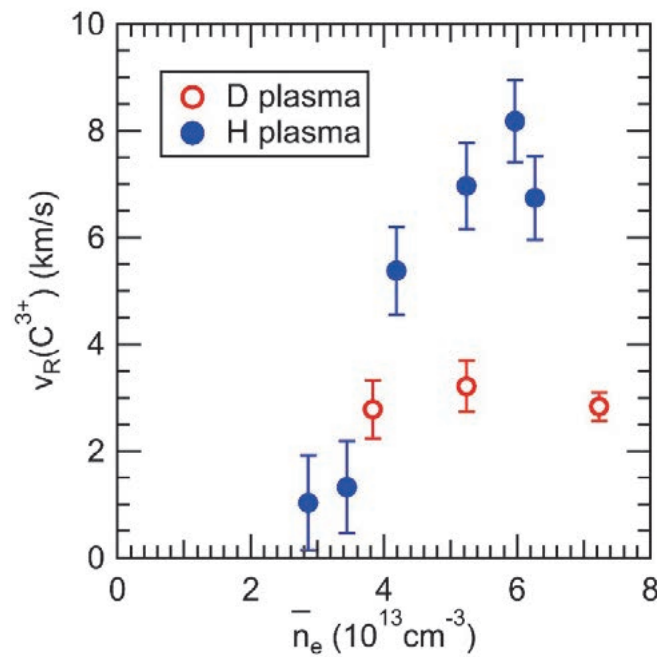


Fig. 2 Observed C^{3+} flow at the bottom edge of the ergodic layer in the D and H plasmas as a function of line-averaged electron density for $R_{ax} = 3.6$ m.

[1] T. Oishi *et al.*, Plasma **6**, 308–321 (2023).

(T. Oishi)

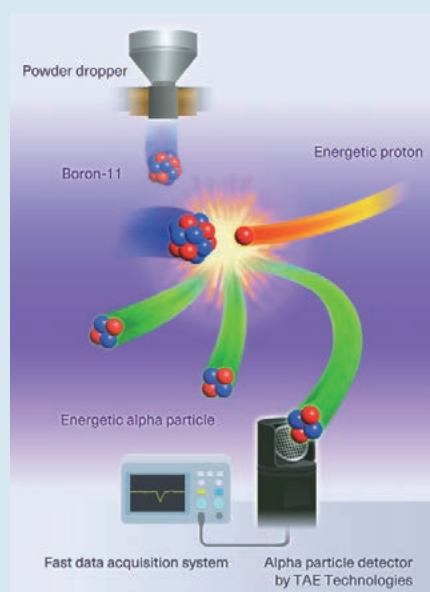
Instability

Highlight

Demonstration of fusion reactions using advanced fusion fuels

In recent years, research toward cleaner fusion reactors has been active, especially among venture companies from around the world. Cleaner fusion reactors will use advanced fusion fuels, which are more difficult to fuse than deuterium and tritium ones, but do not produce neutrons. A hydrogen and boron-11 reactor is possible using energetic hydrogen beams, and the research for this has been led by TAE Technologies. To efficiently cause a fusion reaction, protons must collide with boron-11 at a speed of more than 15,000,000 km/h. The LHD is equipped with the world's only operational hydrogen beam injectors that can shoot the hydrogen into plasma at speeds exceeding 15,000,000 km/h and a powder dropper that can inject boron into plasma. These enable fusion reactions between protons and boron-11 in a magnetically confined plasma.

The fusion reaction between protons and boron-11 produces energetic helium. To demonstrate the reaction, the energetic helium must be detected. The amount of helium produced, and its trajectories are predicted based on numerical simulations, validated in LHD experiments. An alpha particle detector based on a large area semiconductor detector was placed near the surface of the plasma where the energetic helium was predicted to appear. As a result of an experiment in which an energetic hydrogen beam was injected into the boron-sprinkled plasma, energetic helium produced by the fusion reaction between protons and boron-11 was successfully detected, as predicted. This was the world's first demonstration of a fusion reaction between protons and boron-11 in a magnetic confinement fusion plasma. The results of this research are a major first step toward the realization of a cleaner magnetic confinement fusion reactor.



Proton and boron-11 experiment in LHD

(R. M. Magee)

First Observation of Ion Cyclotron Emission from fusion-born protons in a heliotron-stellarator plasma [1]

Ion cyclotron emission (ICE) from fusion-born protons has been observed for the first time in a heliotron-stellarator. During perpendicular deuterium beam injection in the LHD, intense bursty emissions were detected just after the onset of the tongue event that caused a magnetic reconnection and resulted in the exhausting of high energy ions (Fig. 1). We found successive ICE spectral peaks have a typical frequency spacing of 26.6 MHz, comparable to the proton cyclotron frequency in the plasma peripheral region. We stress that these peaks are not located close to the integer multiples of cyclotron frequency but shift from the 8th to 12th. cyclotron harmonics by approximately half the proton cyclotron frequency.

Based on the assumptions that a bursting ICE signal originates from fusion-born ions, at a single location to be identified with the magnetic field strength, under a single collective plasma physics process of the magnetoacoustic cyclotron instability, fusion-born protons which have a perpendicular velocity (v_{\perp}) approximately equal to Alfvén velocity (V_A) and a parallel velocity (v_{\parallel}) approximately 2.4 times V_A might be responsible for the measured frequency shift of the ICE, propagating almost perpendicular to the magnetic field. First principle computations of the collective relaxation of a proton subpopulation near its birth energy $E_H=3.02$ MeV, within a majority thermal deuterium plasma, were carried out using a particle-in-cell approach. We found substantial frequency shifts in the peaks of the simulated ICE spectra, which corresponded closely to the measurement.

This first probable detection of collective electromagnetic radiation from fusion-born ions in a stellarator-type plasma is an encouraging development for magnetically confined (MCF) plasma physics, and shows the flexibility of the LHD heliotron-stellarator and its diagnostic systems. The foregoing is also an example of the reconstruction of the zeroth-order features of the velocity space distribution function of an energetic ion population, based solely on ICE measurements, which reinforces the case for the adoption of ICE as a fast ion diagnostic in ITER.

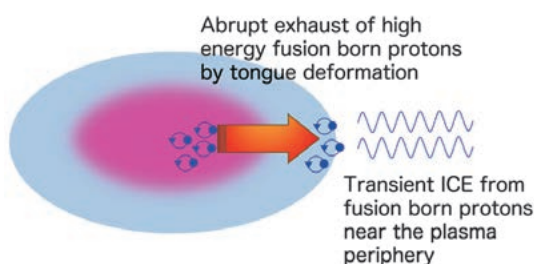


Fig. 1 By abrupt tongue deformation of the confinement magnetic field, transient ICE from fusion born protons which are exhausted from the plasma central region.

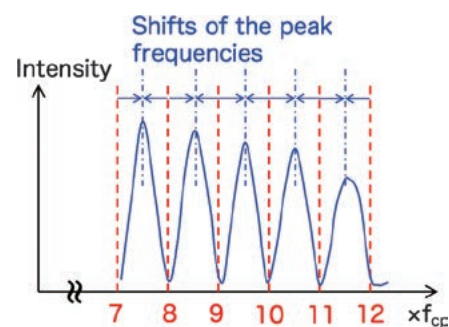


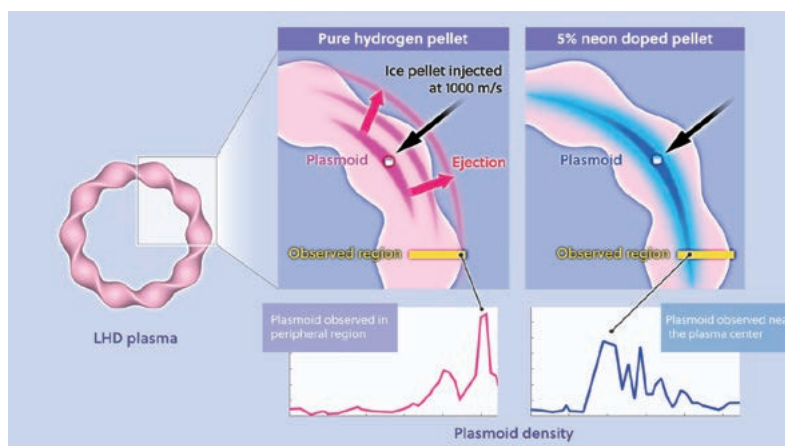
Fig. 2 Successive ICE spectral peaks shift from the integer multiples of proton cyclotron frequency at the likely emitting region.

[1] B C G Reman, R O Dendy, H Igami, T Akiyama, M Salewski, S C Chapman, J W S Cook, S Inagaki, K Saito, R Seki, M Toida, M H Kim, S G Thatipamula and G S Yun, "First observation and interpretation of spontaneous collective radiation from fusion-born ions in a stellarator plasma" *Plasma Phys. Control. Fusion* **64**, 085008 (2022). <https://doi.org/10.1088/1361-6587/ac7892>

Cooling 100 million degree plasma with hydrogen–neon mixture ice pellet injection

At ITER – the world’s largest experimental fusion reactor, currently under construction in France – a so-called “disruption” poses a major open issue. Disruptions are the abrupt termination of magnetic confinement, which causes high-temperature plasma to flow into the inner surface of the containing vessel. Therefore, a dedicated machine-protection strategy is required as a safeguard. As a baseline strategy, researchers are developing a method using ice pellets and injecting them into a high-temperature plasma. The injected ice melts from the surface and evaporates and ionizes owing to heating by the ambient high-temperature plasma, forming a layer of low-temperature high-density plasma (hereafter referred to as a “plasmoid”) around the ice. Such a low-temperature, high-density plasmoid mixes with the main plasma, the temperature of which is reduced during the process, thereby mitigating the heat load to the plasma-facing material components.

However, in recent experiments, it has been observed that when pure hydrogen ice is used, the plasmoid is ejected before it can mix with the target plasma, making it ineffective for cooling the high-temperature plasma deeper below the surface. A solution to this problem was proposed based on an LHD experiment [1]. In the LHD, we discovered that by adding approximately 5% neon to a hydrogen ice pellet, it is possible to cool the plasma more deeply below its surface, and hence, more effectively than when pure hydrogen ice pellets are injected. This result is consistent with model calculations [2], which predict that by mixing a small amount of neon into hydrogen, the internal energy of the plasmoid can be emitted as photon energy, resulting in a suppression of the outward drift motion experienced by the plasmoid. This effect of neon doping is not only interesting as a new experimental phenomenon, but will also contribute to the establishment of plasma control technologies for future fusion reactors.



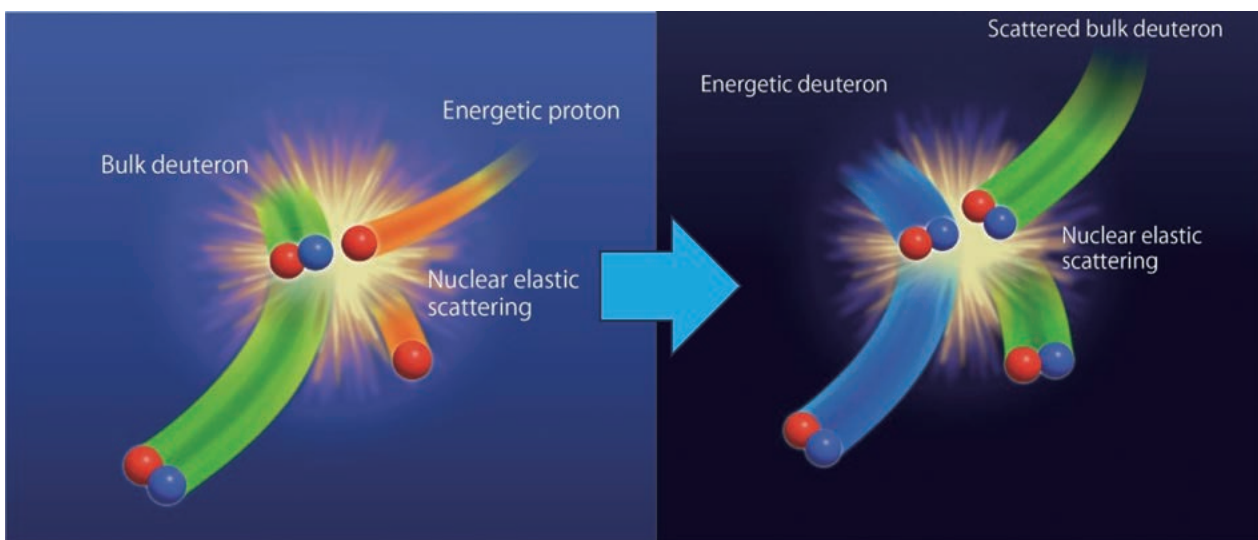
Plasmoid behavior of pure hydrogen and hydrogen mixed with 5 % neon. In this experiment, a new Thomson Scattering (TS) diagnostic system operating at (an unprecedented rate of) 20 kHz was used to (i) measure the density of the plasmoid at the moment it passed through the observation region and (ii) identify its position, which verified the theoretical predictions.

[1] A. Matsuyama, R. Sakamoto, R. Yasuhara *et al.*, Phys. Rev. Lett. **129**, 255001 (2022).

[2] A. Matsuyama, Phys. Plasmas **29**, 042501 (2022).

Observation of energy transfer due to nuclear elastic scattering

Coulomb scattering is usually regarded as the dominant process in the ion collisions in a fusion plasma. However, as the energy of the ions increases, the nuclear elastic scattering due to the ‘nuclear force’, the force becomes non-negligible. Coulomb scattering has a small scattering angle and a small energy transfer per collision, whereas nuclear elastic scattering has a large scattering angle and a large energy transfer per collision. Nuclear elastic scattering has the effect of enhancing ion heating and changing the distribution function of ions, which is expected to improve fusion reactivity in future fusion reactors. In the LHD deuterium plasma experiments, the research group injected deuterium and hydrogen beams simultaneously into the deuterium plasma and analyzed the neutron emission rate and decay time. The neutrons are mainly due to the reaction between bulk deuterons and energetic deuterons. The decay time of the neutron emission rate reflects the change in the velocity distribution of the energetic deuterons. The decay time of the neutron emission rate obtained in the experiment is longer than that predicted by the numerical simulation considering only Coulomb scattering. Energy transfer between energetic ions cannot be explained only by the Coulomb scattering process. To understand the energy transfer between energetic ions, a numerical analysis was carried out using a Boltzmann-Fokker-Planck simulation, in which a Boltzmann collision term describing nucleoplasmic scattering was added to the Fokker-Planck analysis model, which analyses the distribution function of the plasma. The results show that energy is transferred from the energetic protons to the energetic deuterons via the bulk deuterons. Since nuclear elastic scattering has a large energy transfer per collision, the energy transfer by nuclear elastic scattering becomes equivalent to the energy transfer by Coulomb scattering. This result might provide an important insight into the efficiency of power generation in future fusion reactors.



Energy transfer from energetic proton to energetic deuteron via bulk deuteron by nuclear elastic scattering

(H. Matsuura)

Research and Development Collaboration Program for LHD-Project

Highlight

Reduction of co-extracted electron current owing to expansion of deuterium negative-ion plasma region

Negative-ion source-based neutral beam injection (NBI) has the problem that the electron current co-extracted from deuterium plasma is higher than that from hydrogen plasma. A deflection magnetic field is applied near the plasma grid (PG), and an ionic plasma composed of positive and negative ions is maintained near the PG surface. Here, negative ions are produced by irradiating a PG made of aluminum (Al-PG) with hydrogen/deuterium plasma without caesiation. The irradiation surface is set to the axial position of -1.3 cm. Plasma axial distributions are measured by a Langmuir probe when deflecting magnets are embedded inside the Al-PG (the magnet center at -0.8 cm). Figure 1 (a) shows the axial distributions of the probe negative/positive saturation-current ratio, depending on the DC voltage biased to the Al-PG. The current ratio is about 30 or more in the discharge plasma and around one in the ionic plasma. The boundary region of the ionic plasma has a current ratio of 2–3, and the boundary position changes depending on the Al-PG voltage. For Al-PG voltage higher than $+2$ V, the ionic plasma is maintained at -2.3 cm. For Al-PG voltage lower than $+2$ V, the electron-rich region (the current ratio higher than 3) is in the discharge plasma and downstream from the Al-PG aperture. It has been clarified that these electrons downstream are not the co-extracted electrons derived from the discharge plasma but detached electrons that appear after precursor ions decay. The axial distributions of the current ratio at the Al-PG voltage of $+2$ V are shown in Fig. 1 (b). When the deflection magnet center is at -4.9 cm, the ionic plasma is maintained downstream from -6.5 cm, and the volume of the ionic plasma significantly increases. The current ratio is higher than 18 without the magnets, and no ionic plasma region is formed. Regardless of the position of the magnet center, the deflection magnetic-flux density is 22 mT at the boundary position. The co-extracted electron current is suppressed when the meniscus near the Al-PG aperture is far from the boundary region.

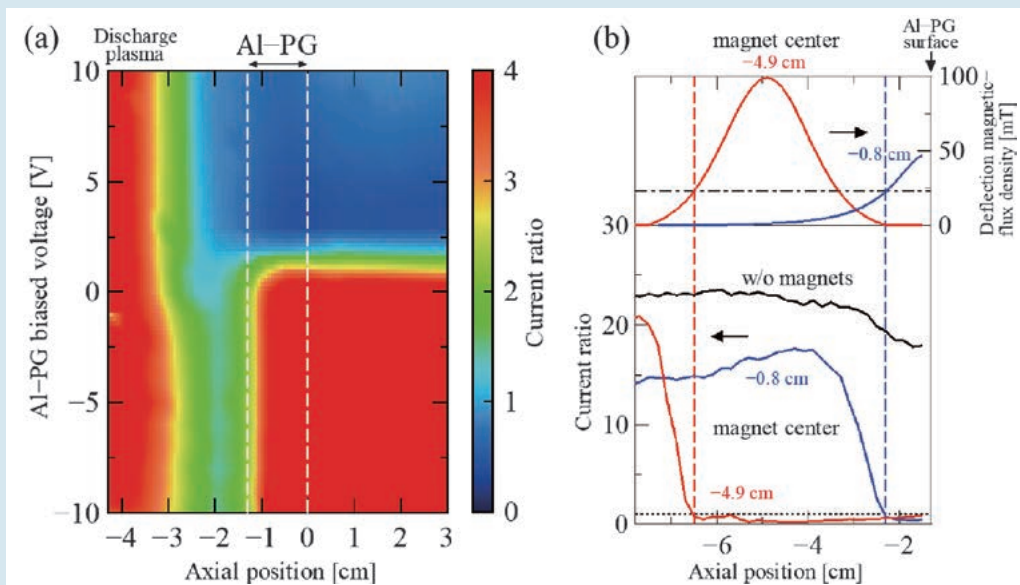


Fig. 1 (a) Axial distributions of probe negative/positive saturation-current ratio depending on DC voltage biased to Al-PG, (b) axial distributions of current ratio and deflection magnetic-flux density at Al-PG voltage of $+2$ V.

(W. Oohara)

Development of ghost imaging absorption spectroscopy and observation of 3-D structure of detached plasma

We are developing a ghost imaging absorption spectroscopy method by integrating computational ghost imaging (CGI) with plasma absorption spectroscopy. Ghost imaging is a method that employs a single-pixel detector such as a photodiode to capture an image of an object [1]. Figure 1 shows schematics of a CGI absorption spectroscopy system. A random intensity pattern, $I_r(x,y)$, is computationally generated by a personal computer, and the structure is transcribed to an illumination laser using a digital micromirror device (DMD). As depicted in Fig. 1, the structured light is absorbed by plasma with a transmittance distribution $T(x,y)$. A lens focuses the transmitted light onto a photodiode, and its total intensity b_r is measured. The value of $T(x,y)$ is subsequently computed as follows:

$$T(x,y) = \frac{\langle b_r I_r(x,y) \rangle - \langle I_r(x,y) \rangle \langle b_r \rangle}{|\langle I_r(x,y) \rangle|^2}, \quad (1)$$

where $\langle \dots \rangle$ denotes an average over independent structured light patterns. By switching and averaging tens of thousands of $I_r(x,y)$ patterns, the contrast of the resultant $T(x,y)$ is incrementally improved. As this imaging method is predicated on the correlation between b_r and $I_r(x,y)$, it exhibits a noise tolerance analogous to lock-in detection. Moreover, by restricting the area of correlated absorption with $I_r(x,y)$ through the focusing of structured light, spatial resolution in the line-of-sight can be attained even in absorption spectroscopy.

The newly developed spectroscopy system has been employed to visualize the distribution of metastable helium atoms near the plasma endplate of a helicon-wave plasma device. Figure 2(a) presents a side-view image of the device, showing the plasma generated upstream of the device on the right side being terminated at the end plate. Structured lights illuminate a $27 \text{ mm} \times 17 \text{ mm}$ area indicated by the red square.

Figure 2(b) shows metastable helium distribution. The numbers on the horizontal and vertical axes represent the number of pixels in the image. The surface of the end plate is located around 40 on the horizontal axis, and an increase in the metastable density is observed towards the upstream of the device. Since the principle of CGI absorption spectroscopy has been verified, we intend to employ this measurement method to obtain the distribution of metastable atoms in detached plasmas.

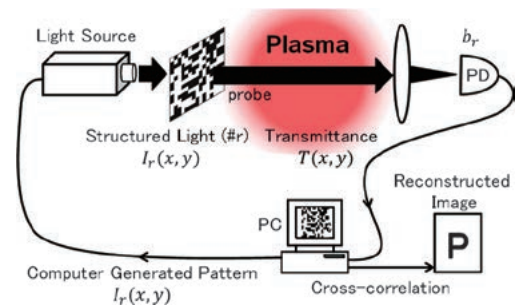


Fig. 1 Schematics of CGI absorption spectroscopy system.

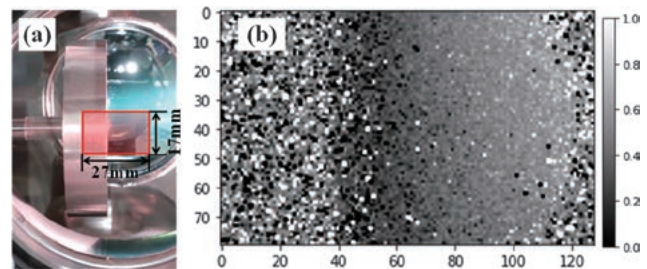


Fig. 2 (a) Measurement area by ghost imaging absorption spectroscopy. (b) Absorption distribution near the plasma end plate.

[1] J. H. Shapiro, Phys. Rev. A **78**, 061802(R) (2008).